IEEE Photonics Journal
An IEEE Photonics Society Publication

Investigations of Backscattering Effects in Optical Fibers and Their Influences on the Link Monitoring

Volume 9, Number 2, April 2017

Qiguang Feng
Wei Li
Qiang Zheng
Jinyao Wang
Haitao Li
Qianggao Hu
Shaohua Yu

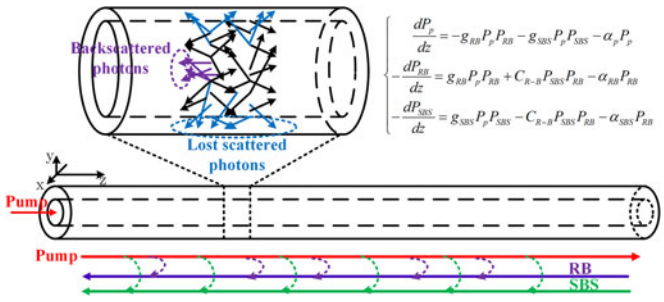

DOI: 10.1109/JPHOT.2017.2682847
1943-0655 © 2017 IEEE

Investigations of Backscattering Effects in Optical Fibers and Their Influences on the Link Monitoring

Qiguang Feng,[1] Wei Li,[1] Qiang Zheng,[1] Jinyao Wang,[1] Haitao Li,[2] Qianggao Hu,[2] and Shaohua Yu[3]

[1]Wuhan National Lab for Optoelectronics, Huazhong University of Science and Technology, Wuhan 430074, China
[2]Accelink Technologies Company Ltd., Wuhan 430205, China
[3]Wuhan Research Institute of M.P.T., Wuhan 430074, China

DOI:10.1109/JPHOT.2017.2682847

Manuscript received December 1, 2016; revised March 9, 2017; accepted March 13, 2017. Date of publication March 15, 2017; date of current version April 10, 2017. This work was supported in part by China 863 project (2015AA017002), in part by Research Foundation of Wuhan Science and Technology Bureau under Grant 2015010303010141, and in part by Open Foundation of the Accelink Technologies Company Ltd. Corresponding author: Wei Li (e-mail: weilee@hust.edu.cn).

Abstract: In this paper, first, we employed the coupled-mode theory to investigate the backscattering power characteristics of Rayleigh backscattering (RB) and stimulated Brillouin scattering (SBS) both synchronously and precisely. We discovered how the RB and SBS power changed with pump powers and fiber lengths. The scattering power curves with different pump powers could be divided into three regions. The first was called "the linear region of RB," in which the pump power was mainly converted into RB and the RB power grew linearly with pump powers. The second region was called "the stimulation region of Brillouin scattering," in which the power was mainly converted into SBS. In "the gain-saturated region," when the pump power was much higher than the SBS threshold, both the RB and SBS power were gain-saturated. We also obtained the power curves with different fiber lengths. The power curves were helpful to set up proper launch powers in practical engineering applications, such as optical time-dome reflectometry systems and distributed fiber sensors. Then, we verified our theoretical results by experiments. Finally, according to the measurements and numerical solutions of the coupled-mode equations, we discussed the application of backscattering and gave advice for pump power selections in different fiber link monitoring systems.

Index Terms: Rayleigh backscattering (RB), stimulated Brillouin scattering (SBS), optical time-domain reflectometry (OTDR), fiber monitoring, distributed fiber sensor.

1. Introduction

The random optical backscattering effects in fibers including Rayleigh backscattering (RB) and stimulated Brillouin scattering (SBS) were important for practical engineering applications such as the fiber link monitoring and the distributed fiber sensing [1]–[10]. The conventional optical time-domain reflectometry (OTDR) measured the loss traces and detected the fault location in the fiber by transmitting short optical pulses and analyzing their backscattering signals [2]. The Brillouin OTDR (B-OTDR) utilized the frequency shift of SBS to measure the location of the fault and the distance of the optical network units (ONUs) [3]. The in-service correlation OTDR employed the backscattering light of downstream signals to realize the fiber link monitoring and the fault location in high split-ratio

passive optical network (PON) systems [4]–[6]. In particular, the OTDRs could also be used in long-haul WDM transmission link, including cascaded in-line EDFAs, in which the influences of RB and SBS lights were greater [7].With the distance and split-ratio extensions in PON systems, the power of the probe light would be higher. The characteristics of RB, SBS and their interactions were significant for the performance of OTDRs, such as the dynamic range, the sensitivity and the fault location accuracy. Some distributed fiber sensing systems are also based on Rayleigh and Brillouin scatterings [8]–[10]. For instance, the hybrid Φ/B-OTDRs which took advantage of both the Rayleigh and Brillouin backscattering, had better performance for simultaneous vibration and strain measurements [10]. Besides, RB and SBS noise could cause gain and modal instability in fiber amplifiers and lasers [11]. In those systems, the characteristics of backscattering lights including RB and SBS changed with pump powers, fiber types and lengths. Therefore, it was meaningful to present a precise model to analyze the characteristics of backscattering synchronously and precisely.

In recent years, researchers had made a lot of studies on power characteristics and influences of RB and SBS in optical fiber systems. For instance, Gysel *et al*. [12] studied the power density spectrum of RB in the fiber with different linewidth lasers. They explained the phenomenon with statistical properties of scattering sources. Okusaga *et al*. [13], [14] proposed the entropy mode theory and explained how the RB spectrum changed with fiber lengths [13]. Besides, they had observed the super linear growth of the RB power with the launch power [14]. Kobyakov *et al*. [15] analyzed the spectrum and power characteristics of SBS and introduced the influence of SBS on different fiber systems.

However, most of the above previous researchers investigated the power characteristics of RB and SBS in isolation [12]–[15]. They neglected the possibility of the interaction between RB and SBS. Only the coupling between the RB light and the pump light or the coupling between the SBS light and the pump light had been taken into account in the above previous research. In the actual fiber system, the RB accompanied with the SBS. It was unclear how RB and SBS impacted the system cooperatively. Moreover, the above previous theories were based on statistical optics and the results were not very precise. Therefore, it was necessary to build up an accurate and uniform model describing properties of the interaction among RB, SBS and pump lights. It was significant to analyze the influences of RB and SBS synthetically and precisely.

In this paper, based on coupled-mode theory, we proposed the coupled-mode equations of these three lights: the pump light, RB light and SBS light at the same time. We adopted numerical analysis method to get the accurate solutions of the coupled-mode equations and investigated how RB power and SBS power changed with fiber lengths and pump powers. Based on the model, we could precisely analyze power interactions among these three lights: RB, SBS, and pump light.

Then, we measured RB powers and SBS powers with different fiber lengths and pump powers. Different from other investigators only testing the total scattering power in their experiments [12]–[15], we selected the peak power at 1550 nm as the power of RB and the peak power at about 0.1 nm longer wavelength as the power of SBS, which could represent the intensity of RB and SBS more accurately. Moreover, we noticed that the total backscattering power grew with pump powers linearly in the saturated region. It may potentially be used for a novel kind of “enhanced Brillouin link monitors,” which has very high backscattering power and can realize long-reach fiber link detection without using APD or coherent detection *etc*.

The rest of this paper is organized as follows. In Section 2, we introduce the coupled-mode theory of RB, SBS and pump light. Section 3 is the experimental setup and analysis of the measurements. In Section 4, we conclude the paper.

2. Theory

Fig. 1 is the schematic diagram of the random scatterings in fibers, including Rayleigh scattering and Brillouin scattering. As shown in Fig. 1, the pump light transmits along the forward direction of the z axis and is scattered randomly. A little part of the scattering photons can transmit along the backward direction of the z axis, which are called Rayleigh backscattered photons. The Rayleigh backscattering (RB) is just induced by the Rayleigh backscattered photons [1]. The RB light transmits

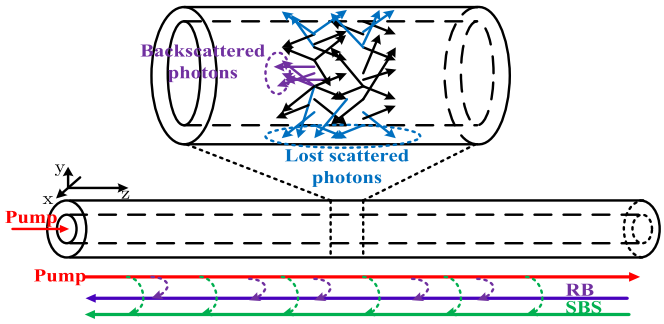

Fig. 1. Schematic diagram of RB and SBS in the fiber and their coupling with the pump light.

along the backward direction of the z axis with the same wavelength as the pump light. Besides, the pump light interacts with the acoustic field in the fiber to generate the backward Brillouin scattering light. At high pump powers, the Brillouin scattering can be converted into a stimulated process [15].

Most of the previous researchers investigated the power characteristics of RB and SBS in isolation [12]–[15]. Only the coupling between the RB light and the pump light or the coupling between the SBS light and the pump light had been taken into account in their researches. That resulted in the neglect of the possibility of the interaction between RB and SBS. With all these assumptions, the RB power is expressed as [14]

$$\begin{cases} \frac{dP_p}{dz} = -g_{RB}P_pP_{RB} - \alpha_pP_p \\ -\frac{dP_{RB}}{dz} = g_{RB}P_pP_{RB} - \alpha_{RB}P_{RB}. \end{cases} \tag{1}$$

In (1), P_p is the power of forwards pump light and P_{RB} is the power of RB. g_{RB} is the gain factor related to the interaction between pump light and RB. α_p and α_{RB} are the attenuation factors of the pump light and Rayleigh scattering light in the fiber. In SSMF, the RB light has the same wavelength with the pump light, and therefore there is $\alpha_{RB} = \alpha_p = \alpha$. When the pump depletion is neglected, the solution of RB in(1) can be expressed as

$$P_{RB}(0) = P_{RB}(z)\, e^{\frac{g_{RB}P_p(0)L_{eff}}{A_{eff}} - \alpha z} \tag{2}$$

where $P_{RB}(z)$ denotes the power of RB seed light generated at the coordinate z, $P_{RB}(0)$ denotes the power when the seed light transmits to the receiver at the position z = 0, A_{eff} is the effective core area, and L_{eff} is the effective interaction length. For RB, the index $\frac{g_{RB}P_p(0)L_{eff}}{A_{eff}}$ was extremely less than "1". Therefore, we observed the RB power grew linearly with the pump power in general cases.

If only considering the coupling between the Brillouin light and pump light, the coupled-mode equations of them can be written as [15]

$$\begin{cases} \frac{dP_p}{dz} = -g_{SBS}P_pP_{SBS} - \alpha_pP_p \\ -\frac{dP_{SBS}}{dz} = g_{SBS}P_pP_{SBS} - \alpha_{SBS}P_{SBS}. \end{cases} \tag{3}$$

In (3), P_{SBS} is the power of SBS. g_{SBS} is the gain factor related to the interaction between the pump light and SBS.

Based on the investigation of Kobyakov *et al.* [15], when the pump depletion can be neglected, the SBS power can be expressed as

$$P_{SBS}(0) = P_{SBS}(L)\, e^{\frac{g_{SBS}P_p(0)L_{eff}}{A_{eff}} - \alpha L}. \tag{4}$$

As shown in (4), the SBS power increases with the pump power exponentially and the threshold of SBS can be calculated from (4).

With the above previous methods, we can analyze the power characteristics of RB and SBS conveniently but there are still some limitations of those methods. First, only the coupling

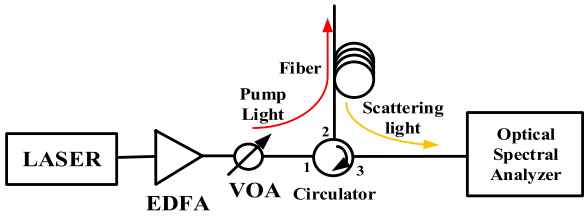

Fig. 2. The schematic diagram of our experimental setup.

between one backward light and the pump light had been taken into account in the above previous researches, but in the actual fiber system, the RB light accompanies with the SBS light. RB and SBS should be included in the equations at the same time. Secondly, the model cannot describe the power saturation processes of SBS and RB lights. The models are ineffective at high pump power, because the pump depletion is not taken into account. Thirdly, the possibility of the interaction between RB and SBS was neglected.

Therefore, we proposed the coupled-mode equations of the pump light, the RB light and the SBS light, considering the interactions among all the three light at the same time. Based on the coupled-mode theory, our modified coupled-mode equations are expressed as

$$\begin{cases} \frac{dP_p}{dz} = -g_{RB}P_pP_{RB} - g_{SBS}P_pP_{SBS} - \alpha_pP_p \\ -\frac{dP_{RB}}{dz} = g_{RB}P_pP_{RB} + C_{R-B}P_{SBS}P_{RB} - \alpha_{RB}P_{RB} \\ -\frac{dP_{SBS}}{dz} = g_{SBS}P_pP_{SBS} - C_{R-B}P_{SBS}P_{RB} - \alpha_{SBS}P_{RB} \end{cases} \tag{5}$$

where C_{R-B} is the coupled coefficient to describe the interaction between the RB and the SBS. We can get the values of g_{RB}, g_{SBS} and C_{R-B} by calculating the overlap integrals between any two transverse modes of the three lights. In standard single-mode fibers (SSMF), the wavelength of RB is the same as the wavelength of the pump and the frequency of Stokes SBS is only about 10.8 GHz lower than that of the pump light, so there is $\alpha_{SBS} \approx \alpha_{RB} = \alpha_p = \alpha$.

There are three advantages of our proposed model. First, the interactions among RB, SBS and the pump light are all included in our model, which can describe the actual coupling proceeding among these three lights more precisely. Second, the coupling between the RB light and the SBS light is considered, which could make the numerical solutions fit with the experimental measurements much better. Thirdly, we adopt numerical analysis methods to get the precious solutions of (5), which is helpful to investigate the conversion of the optical powers among these three lights more adequately.

Especially, we neglected the influence of the lights' phase variation in the coupled-mode equations. When the measured fiber lengths were longer than the coherent length of the laser, our model could precisely describe the power transfer among the pump, RB and SBS lights. But when the measured fiber lengths were shorter than the coherent length of the laser, there were some phenomena being not able to be expressed, such as the experiments of Zhu *et al.* [16].

Based on our model, we simulated how the RB power and the SBS power changed with fiber lengths and pump powers by numerical methods. In the next section, we compared our numerical solutions with the experimental measurements.

3. Experiments and Analysis

Fig. 2 shows the schematic diagram of the experimental setup that we verified our model. The light from an about 100 kHz linewidth laser at 1550 nm was fed into the fiber by an EDFA, a variable optical attenuator (VOA) and an optical circulator. The VOA and EDFA were used to adjust the launch power of the forward pump light. Through the same optical circulator, the backscattering light was sent to an optical spectral analyzer, where we measured the optical spectrum. The fiber we used was SMF-28e. Its attenuation is about 0.18 dB/km and the mode field diameter is about

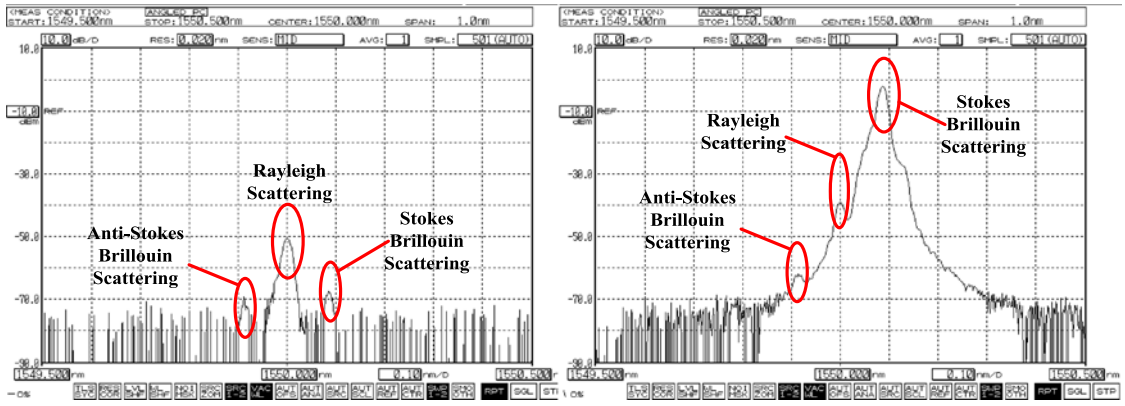

Fig. 3. Backscattering spectra of 20 km fiber when pump light powers are at (a) 3 dBm and (b) 16 dBm.

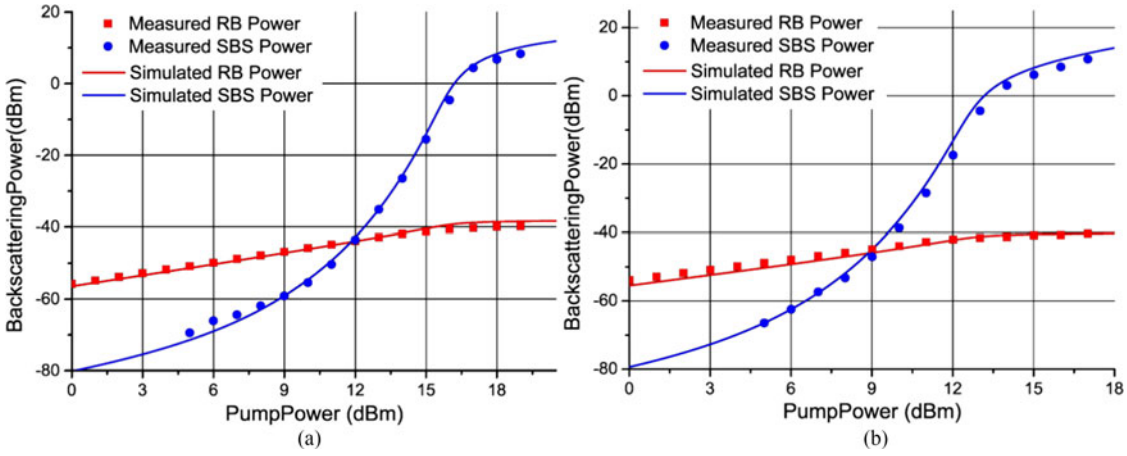

Fig. 4. RB power and the SBS power vs. pump powers when fiber lengths are (a) 5 km and (b) 10 km.

10.4 um at 1550 nm. In our simulation based on coupled-mode equations, the parameters were consistent with SMF-28e. Different from other investigators testing the total scattering power in their experiments [10]–[12], we selected the peak power at 1550 nm as the power of RB and the peak power at 0.1 nm (10.8 GHz) longer wavelength as the power of SBS, which could represent the intensity of RB and SBS more accurate.

Fig. 3(a) and 3(b) are the optical spectra of the backscattering light of 20 km SSMF at 3 dBm and 16 dBm pump powers, respectively. The data highlight three kinds of spectra: the spectral region around the wavelength of the incident light, and the regions about 0.1 nm above and below the wavelength of the incident light. The latter two regions correspond to the anti-Stokes and the Stokes lights induced by Brillouin scattering. As shown in Fig. (3), the power of Stokes Brillouin scattering is much higher than that of anti-Stokes scattering with increasing of the pump power. So, we selected the peak power of the Stokes wave standing for the intensity of Brillouin scattering and the peak power at 1550 nm standing for the intensity of RB [9]. At 3 dBm pump power, the RB power is about 20 dB higher than the Stokes Brillouin scattering power, so the backscattering was mainly Rayleigh scattering. In contrast, at 16 dBm pump power, the SBS power is over 30 dB higher than the RB, and therefore, the SBS was the principal process of backscattering.

Then, we measured how the RB power changed with pump powers and fiber lengths. The results are shown in Figs. 4 and 5. The fiber lengths are 5 km, 10 km, 20 km, and 50 km, respectively.

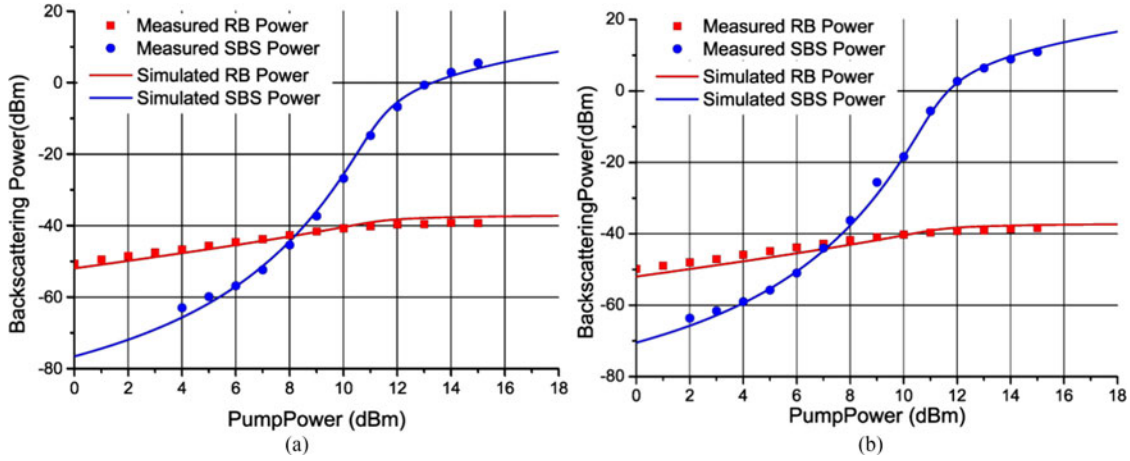

Fig. 5. RB power and the SBS power vs. pump power when fiber lengths are (a) 20 km and (b) 50 km.

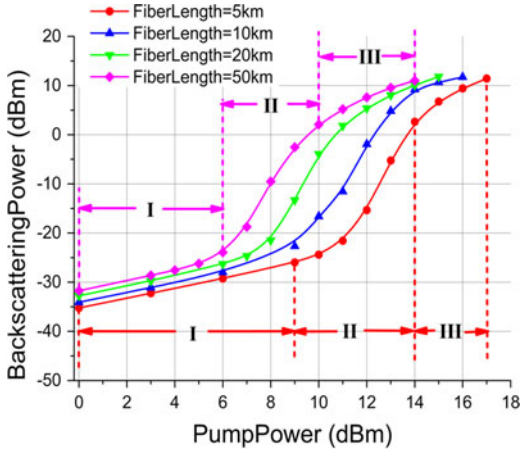

Fig. 6. Total backscattering power vs. pump power with different fiber lengths.

The linewidth of the laser in the experiment is 1 MHz and its coherent length is about 200 m. So, the measured fiber lengths are longer than the coherent length of the laser. The red diamonds are the measurements of the RB peak power at 1550 nm of backscattering spectrum acquired by optical spectral analyzer. The blue spheres are the measurements of the SBS peak power at about 1550.1 nm. The red and blue curves are the numerical solutions of RB power and SBS power, according to the coupled-mode equations [see (1)].

According to Figs. 4 and 5, the RB power increases with the pump power linearly and the SBS power increases with the pump power exponentially, when the pump power is low. The conclusions are consisted of previous researches which are described with (2) and (4). However, at extremely high pump power, both of the RB power and the SBS power are gain-saturated. The gain-saturated pump powers decrease with the increase of the fiber length. The gain-saturations should be attributed to the pump depletion. But the saturated pump power of RB is different from that of SBS, which can be induced by the differences between the gain factors of RB and SBS (g_{RB} and g_{SBS}).

Replacing the spectrum analyzer with an optical power meter, we measured how the total backscattering power changed with pump powers and fiber lengths. As shown in Fig. 6, all the total power curves can be divided into three regions: Region I, the process of Rayleigh backscattering, Region II, the stimulated process of Brillouin scattering, and Region III, the process of power saturation.

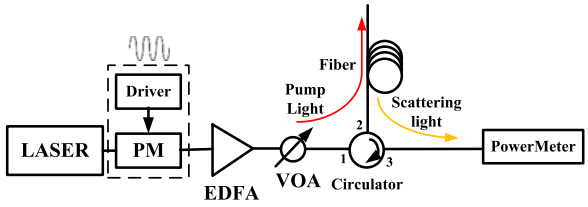

Fig. 7. Investigations on how the pump phase modulation influence the backscattering power.

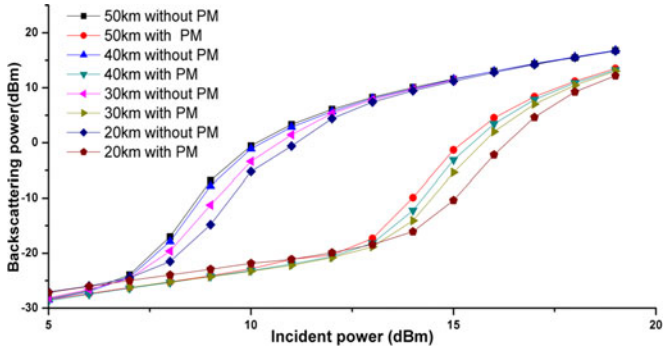

Fig. 8. Total backscattering power for different pump powers and fiber lengths.

4. Discussion on the Application of Backscattering

In the first region, the scattering power was mainly from RB and increased with pump powers linearly. The region had been applied to conventional OTDRs and in-service OTDRs for fiber link detections. The linearity of RB was important for precise attenuation measurements and fault locations. To get wider dynastic range at low detection sensitivity, the pump power should be set at the highest power of the first region. According to our model and experiments, the range of the linear region was determined by the fiber length and the threshold of SBS. The threshold of SBS was the main limiting factor. It could mitigate SBS and improve its threshold to modulate the phase of the pump light. Therefore, to expand the power range of the linear region, we could modulate the phase of the pump light using a low frequency modulation such as a sine signal to mitigate the SBS. The linewidth of the laser used in conventional OTDR was usually to be several MHz [17]. The coherent length of the laser was shorter than the length of tested fibers and the phase of RB was completely random. Therefore, the phase modulation would not change the linearity power characteristics of RB. Besides, the phase modulation could decrease the gain factor related to the interaction between the pump light and SBS (g_{SBS}) to improve the threshold of SBS [1], [17].

Fig. 7 shows the experimental setup that we expanded the range of the linear region by pump phase modulation. The phase modulator (PM) was inserted between the laser and the EDFA and the driving signal was 200MHz sine signal. Then, the power meter was used to measure the backscattering power. Adjusting the VOA to change the pump power, we measured the backscattering power curves with different fiber lengths.

Fig. 8 shows the backscattering power with different pump powers and fiber lengths. When there was no phase modulation, the threshold was about 6 dBm for 50 km and 7 dBm for 20 km, respectively. In contrast, when the incident light was phase modulated, SBS was mitigated and the threshold increased to about 12 dBm and 13 dBm for 50 km and 20 km fibers, respectively. The linear region was expanded about 6 dB and it was effective for the phase modulation to improve the threshold of SBS.

The quantitative analysis of this method was firstly presented by Dianov *et al.* [18] and summarized by Agrawal [19]. Assuming the original Brillouin gain is G_{B0}, the bandwidth of SBS is $\Delta\nu_B$, the modulation frequency is $\Delta\nu_m$, the effective Brillouin gain G_{eff} with phase modulation can be

expressed as

$$G_{eff} = \left(1 + \frac{\Delta\nu_m}{\Delta\nu_B}\right) G_{B0}. \quad (6)$$

Because the effective Brillouin gain is reduced by a factor of $(1 + \frac{\Delta\nu_m}{\Delta\nu_B})$, the SBS threshold increases by the same factor. According to the quantitative analysis, when the bandwidth of SBS was 70 MHz and the modulating frequency was 200 MHz in our experiments, the SBS threshold should increase by 7.2 dB, which was almost as much as our experiments.

Thus, the maximum length of the tested fiber could be expanded about 15 km with the fixed detector sensitivity. But the threshold still had a limitation, even the pump light was phase modulated. In order to avoid SBS, the pump power should not be higher than 15 dBm when the fiber length longer than 30 km, even with pump light phase modulation.

In Region II, the Brillouin scattering was stimulated gradually. At the middle part of the second region, the spectrum and frequency of SBS were more sensitive to variations of the vibration and strain. Therefore, in B-OTDRs and Brillouin distributed fiber sensors, the pump power should be set at the middle part of the second region. Moreover, with the increase of the fiber length, SBS was saturated at lower pump power and the power range of Region II became narrower. Thus, in B-OTDRs, with the increase of the fiber length, the pump power should be lower to avoid the power saturation, and in Brillouin distributed fiber sensors, the sensing fiber length should be not too long, in order to guarantee the high sensitivity in wider launch power range.

The third region had hardly been used in optical fiber systems. We noticed that the total scattering power approximately grew up with the pump power linearly, which could be used in the fault detection. For instance, in the long-reach fiber sensing system, the power of the light scattered by the remote nodes was extremely low at the receiver. For the enhanced Brillouin OTDR, the received power would be higher to improve the dynamic range.

Besides, for Rayleigh scattered light measurement, deterioration of OTDR waveform due to optical nonlinear phenomena has been reported for high power input of test light [20], and similar instability is also concerned with Brillouin OTDR measurement. But, for the restriction of our equipment, we had not taken notice of these phenomena. In our future research, we will pay more attention to the influence of nonlinear phenomena.

5. Conclusion

In this paper, we investigated the power characteristics of RB and SBS synchronously and precisely based on coupled-mode equations and measured the accurate RB and SBS powers with the optical spectral analyzer. Then, we compared the measured powers with the numerical solutions of the coupled-mode equations, with different fiber lengths and pump powers. All the measurements were fit well with the corresponding numerical solutions. Analyzing RB and SBS power characteristics with our model is helpful for selecting proper launch powers of PONs and improving the OTDR performance. For the traditional OTDRs and in-service OTDRs based on RB, the pump power should be lower than the SBS threshold. At this time, the backscattering power grows linearly with the pump power, which is helpful for the fiber link fault detection and allocation. For Brillouin OTDR, the pump power should be higher than the threshold and lower than the saturated pump power, which assures steady frequency shift property. In the saturated region, the total backscattering power grows with pump powers linearly, which may be used for link detection in the case of long-reach and high-split-ratio PONs.

References

[1] S. K. Turitsyn *et al.*, "Random distributed feedback fibre laser," *Nature Photon.*, vol. 4, pp. 231–235, 2010.
[2] C. Kuznia *et al.*, "Novel high-resolution OTDR technology for multi-GBPS transceivers," in *Proc. Opt. Fiber Commun. Conf.*, 2014, Paper W1F.2.

[3] N. Honda, D. Iida, H. Izumita, and Y. Azuma, "In-service line monitoring system in PONs using 1650-nm brillouin OTDR and fibers with individually assigned BFSs," *J. Lightw. Technol.*, vol. 27, no. 20, pp. 4575–4582, Oct. 2009.
[4] M. Thollabandi, T.-Y. Kim, S. Hann, and C.-S. Park, "Tunable OTDR based on direct modulation of self-injection-locked RSOA for in-service monitoring of WDM-PON," *Photon. Technol. Lett.*, vol. 20, no. 15, pp. 1323–1325, 2008.
[5] L. Sandstrom, D. Joffe, G. Bekken, J. Brooks, K. Schneider, and R. Goodson, "High performance, in-service correlation OTDR," in *Proc. Opt. Fiber Commun. Conf.*, 2013, Paper OW3G.3.
[6] Y. R. Zhou *et al*., "Field trial demonstration of novel optical super channel capacity protection for 400G using DP–16QAM and DP–QPSK with in-service OTDR fault localization," in *Proc. Opt. Fiber Commun. Conf.*, 2016, Paper W3B.3.
[7] P. Kim *et al*., "Novel in-service supervisory system using OTDR for long-haul WDM transmission link including cascaded in-Line EDFAs," *Photon. Technol. Lett*., vol. 13, no. 10, pp. 1136–1138, 2001.
[8] A. Zornoza, A. Minardo, R. Bernini, A. Loayssa, and L. Zeni, "Pulsing the probe wave to reduce nonlocal effects in brillouin optical time-domain analysis (BOTDA) sensors," *IEEE Sensors J.*, vol. 11, no. 4, pp. 1067–1068, Apr. 2011.
[9] Y. Yu, L. Luo, B. Li, K. Soga, and J. Yan, "Frequency resolution quantification of brillouin-distributed optical fiber sensors," *Photon. Technol. Lett*., vol. 28, no. 21, pp. 2367–2370, 2016.
[10] F. Peng and X. Cao, "A hybrid Φ/B-OTDR for simultaneous vibration and strain measurement," *Photon. Sensors*, vol. 6, no. 2, pp. 121–126, 2016.
[11] A. V. Smith and J. J. Smith, "Mode instability in high power fiber amplifiers," *Opt. Exp.*, vol. 19, no. 11, pp. 10180–10192, 2011.
[12] P. Gysel and R. K. Staubli, "Spectral properties of rayleigh backscattered light from single-mode fibers caused by a modulated probe signal," *J. Lightw. Technol.*, vol. 8, no. 12, pp. 1792–1798, 1990.
[13] O. Okusaga, J. Cahill, A. Docherty, W. Zhou, and C. R. Menyuk, "Guided entropy mode Rayleigh scattering in optical fibers," *Opt. Lett.*, vol. 37, no. 4, pp. 683–685, 2012.
[14] J. P. Cahill, O. Okusaga, W. Zhou, C. R. Menyuk, and G. M. Carter, "Superlinear growth of Rayleigh scattering-induced intensity noise in single-mode fibers," *Opt. Exp.*, vol. 23, no. 5, pp. 6400–6407, 2015.
[15] A. Kobyakov, M. Sauer, and D. Chowdhury, "Stimulated brillouin scattering in optical fibers," *Adv. Opt. Photon.*, vol. 2, no. 1, pp. 1–59, 2010.
[16] T. Zhu, X. Bao, L. Chen, H. Liang, and Y. Dong, "Experimental study on stimulated Rayleigh scattering in optical fibers," *Opt. Exp.*, vol. 18, no. 22, pp. 22958–22963, 2010.
[17] C. M. Zeringue, I. Dajani, and G. T. Moore, "Suppression of stimulated Brillouin scattering in optical fibers through phase-modulation: a time dependent model," in *Proc. SPIE*, vol. 7914, 2011, Paper 791409.
[18] E. M. Dianov, B. Y. Zeldovich, A. Y. Karasik, and A. N. Pilipetskii, "Feasibility of suppression of steady-state and transient stimulated Brillouin scattering," *Sov. J. Quantum Electron.*, vol. 19, no. 8, pp. 1051–1053, 1989.
[19] G. P. Agrawal, "Stimulated brillouin scattering," in *Nonlinear Fiber Optics*, 5th ed. New York, NY, USA: Academic, 2013, Ch. 9.
[20] H. Izumita, Y. Koyamada, S. Furukawa, and I. Sankawa, "The performance limit of coherent OTDR enhanced with optical fiber amplifiers due to optical nonlinear phenomena," *J. Lightw. Technol.*, vol. 12, no. 7, pp. 1230–1238, Jul. 1994.